

Capacity-Aware Inference: Mitigating the Straggler Effect in Mixture of Experts

Shwai He¹ Weilin Cai² Jiayi Huang² Ang Li¹

¹University of Maryland, College Park

²The Hong Kong University of Science and Technology (Guangzhou)

shwaihe@umd.edu, angliice@umd.edu

Abstract

The Mixture of Experts (MoE) is an effective architecture for scaling large language models by leveraging sparse expert activation to balance performance and efficiency. However, under expert parallelism, MoE suffers from inference inefficiencies due to imbalanced token-to-expert assignment, where underloaded experts complete computations early but must wait for overloaded experts, leading to global delays. We define this phenomenon as the *Straggler Effect*, as the most burdened experts dictate the overall inference latency. To address this, we first propose **Capacity-Aware Token Drop**, which enforces expert capacity limits by discarding excess tokens from overloaded experts, effectively reducing load imbalance with minimal performance impact (e.g., 30% speedup with only 0.9% degradation on OLMoE). Next, given the presence of low-load experts remaining well below the capacity threshold, we introduce **Capacity-Aware Expanded Drop**, which allows tokens to include additional local experts in their candidate set before enforcing strict local capacity constraints, thereby improving load balance and enhancing the utilization of underused experts. Extensive experiments on both language and multimodal MoE models demonstrate the effectiveness of our approach, yielding substantial gains in expert utilization, model performance, and inference efficiency, e.g., applying Expanded Drop to Mixtral-8 \times 7B-Instruct yields a 0.2% average performance improvement and a 1.85 \times inference speedup.

1 Introduction

In recent years, the rapid evolution of Large Language Models (LLMs) [32, 38, 11] has driven a wave of innovations, continuously expanding the frontiers of AI research and applications. Among the model architectural innovations, the Mixture of Experts (MoE) framework has emerged as a pivotal technique for optimizing the cost-performance trade-off in LLMs. Specifically, MoE [35, 14] enhances scalability by integrating multiple experts while activating only a subset per input. This selective activation substantially improves model performance without a corresponding increase in computational cost, effectively balancing efficiency and performance.

Despite the success of MoE, a key efficiency challenge lies in the imbalanced token-to-expert distribution, which results in some experts being overloaded while others remain underutilized [26, 46]. In distributed GPU settings, experts are typically sharded across multiple devices, with each GPU responsible for a subset of the experts. Under expert parallelism, low-load experts complete

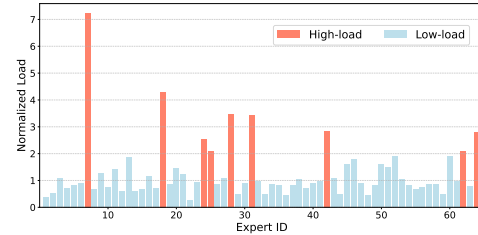


Figure 1: **Illustration of the Straggler Effect in MoE Inference**, where the most burdened experts dictate the overall latency.

their computations earlier but must wait for overloaded experts to finish, as synchronization barriers are required before proceeding to the next stage. This expert-level straggler effect further propagates to device-level delays, where GPUs hosting lighter expert workloads are stalled by GPUs hosting heavier workloads, leading to inefficient resource utilization and increased end-to-end latency during inference. As illustrated in Figure 1, this phenomenon is referred to as the *Straggler Effect*, where the heavily loaded experts determine the overall latency of imbalanced MoE inference.

While auxiliary balance losses have been incorporated into the training process to alleviate imbalance [35, 14, 11], these techniques remain ineffective in mitigating imbalance during inference. Specifically, as shown in Figure 1, our findings reveal a highly uneven token distribution among experts, with the highest-load expert handling more than seven times the expected average load. Moreover, managing such imbalance during inference often incurs additional resource overhead. For example, DeepSeek-V3 mitigates this issue by duplicating high-load experts and deploying them redundantly across devices [11]. This motivates us to explore *efficient token-to-expert assignment* by addressing the key question: *How can we prevent extreme overloading of heavily utilized experts?*

We propose *Capacity-Aware Inference* to address this challenge. Specifically, for high-load experts, we introduce **Capacity-Aware Token Drop**, which imposes a maximum capacity constraint and discards excess tokens from overloaded experts. This approach alleviates severe load imbalance and significantly improves efficiency, while maintaining model performance since the dropped tokens represent only a small fraction of the total workload, e.g., OLMoE achieves a 30% speedup in MoE layers with just a 0.9% performance degradation. After removing excess tokens from overloaded experts, we observe that some low-load experts remain significantly underutilized relative to the predefined capacity constraints, yet must still wait for other experts to complete their computations. This leads us to a second key question: *How can we effectively leverage the available capacity of underutilized experts?*

For low-load experts, we extend Token Drop with **Capacity-Aware Expanded Drop**, which further utilizes the available capacity of underutilized experts to handle overflow tokens from high-load experts. Specifically, under expert parallelism across multiple GPUs, Expanded Drop allows each token to consider additional candidate experts on the same device while still enforcing strict local capacity constraints. This expanded selection improves the utilization of low-load experts and enhances the representational capacity of MoE models under capacity-constrained scenarios.

Extensive experimental results validate the effectiveness of our proposed techniques, demonstrating significant improvements in both efficiency and performance, e.g., *applying Expanded Drop to Mixtral-8×7B-Instruct yields a 0.2% average performance improvement and a 1.85× inference speedup*. Moreover, in multimodal models, we identify redundancy among image tokens and show that applying aggressive capacity constraints (e.g., setting the maximum to half of the average expert load) can still maintain performance. In short, our contributions are in four folds:

- We identify the Straggler Effect caused by token imbalance at inference time in Mixture of Experts, highlighting the optimization potential for reducing latency.
- Toward the high-load experts, we propose **Capacity-Aware Token Drop**, which enforces capacity constraints by discarding excess tokens assigned to overloaded experts, thereby mitigating extreme load imbalance.
- To better utilize underutilized experts, we introduce **Capacity-Aware Expanded Drop**, which expands the candidate expert set to include additional local experts, further improving load balance and model performance.
- Extensive experiments on both language and multimodal models validate the effectiveness of our approach, demonstrating substantial improvements in inference efficiency with comparable performance.

2 Related Works

Mixture of Experts Models The Mixture of Experts (MoE) is a kind of neural network architecture with an extended set of parameters (referred to as “experts”) controlled by a router, which is first introduced in the context of conditional computation [21, 23]. The potential of sparse activation in MoE is subsequently exploited by [34] for efficient training and inference on pretrained models with special designs, opening the door for MoE in various vision [33] and language [25, 13, 14] scenarios. Attributed to its exceptional efficiency, MoE has been adopted as a foundational framework

in the designs of large language models [22, 9, 41, 45, 39], achieving superior scaling laws at low computational costs. Despite these advancements, MoE still faces efficiency challenges in both training and inference [3], and our work specifically focuses on enhancing inference-time efficiency.

Imbalance in Mixture of Experts The imbalance in token-to-expert assignments [44, 5] poses a significant challenge to the deployment of MoE. This imbalance leads to inefficiencies in computation, communication, and memory [18, 37, 42], making it a critical bottleneck for MoE scalability and deployment. To mitigate this issue, an auxiliary balance loss [35] is incorporated into the training process to encourage more uniform token distribution across experts. Additionally, various training strategies have been introduced to further balance token assignments: Switch-Transformer [14] and DeepSeek-V2 [10] implement Token Drop to alleviate expert overload, while DeepSeek-V3 [11] introduces an additional sequence-level auxiliary loss to prevent severe token imbalance.

However, these techniques primarily focus on training and fail to ensure balanced token assignments during inference. Instead, addressing token imbalance at inference often incurs additional resource costs. For example, DeepSeek-V3 [11] mitigates this issue by duplicating high-load experts and deploying them redundantly. In contrast, our approach effectively balances token assignments without introducing additional computational overhead.

3 Background and Motivation

3.1 Extremely Imbalanced Expert Utilization

A Mixture of Experts (MoE) layer consists of a collection of n experts, $\{\mathbf{E}_1, \mathbf{E}_2, \dots, \mathbf{E}_n\}$ and a router \mathbf{G} that dynamically selects the most relevant experts for a given input \mathbf{x} . The router computes selection scores $\mathbf{G}(\mathbf{x})$, for all experts and selects the top k experts, resulting in a sparse activation:

$$\mathcal{K} = \text{TopK}(\text{Softmax}(\mathbf{G}(\mathbf{x})), k). \quad (1)$$

The input \mathbf{x} is processed by the selected experts, and their outputs are combined into a weighted sum based on the router’s scores. This process is mathematically expressed as:

$$\mathbf{y} = \sum_{i \in \mathcal{K}} \mathbf{G}(\mathbf{x})_i \cdot \mathbf{E}_i(\mathbf{x}), \quad (2)$$

where \mathcal{K} denotes the indices of selected experts, $\mathbf{G}(\mathbf{x})_i$ represents the selection score for the i -th expert, and $\mathbf{E}_i(\mathbf{x})$ is the output from the i -th expert. In transformer models, the MoE layer usually replaces the feed-forward network (FFN) and only activates a subset of experts for each input.

While experts in MoE models are often deployed in parallel across distributed GPUs, imbalanced token-to-expert assignments lead to varying levels of expert utilization and potential latency. Despite the incorporation of balancing techniques during training, the load imbalance persists during inference. To further investigate this issue, we conduct preliminary experiments to analyze expert-specific utilization patterns and assess the impact of imbalance on practical latency.

To quantify expert utilization, we measure the load across different experts. Given an input $\mathbf{x} \in \mathbb{R}^{b \times s \times d}$ with batch size b and sequence length s , the total number of tokens is $t = bs$. Since each token selects k out of n experts, the expected token count per expert is:

$$\bar{N} = \frac{tk}{n}. \quad (3)$$

However, due to imbalanced token assignments, some experts may receive more or fewer tokens than the expected value.

Figure 2 illustrates the normalized peak tokens load for each expert to accommodate all tokens within a single layer of OLMoE, where some experts receive an excessively large number of tokens (e.g., more than seven times the average number of tokens), leading to severe load imbalance and, consequently, significant latency. A detailed layer-by-layer analysis is provided in Appendix E.

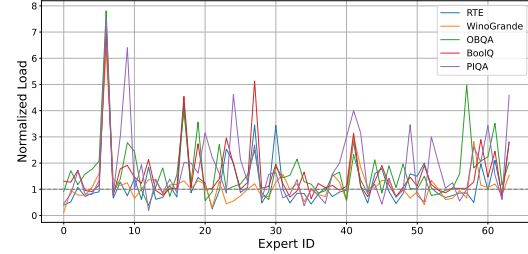


Figure 2: **Expert-wise load**, where each load value is divided by \bar{N} for clarity. To ensure generality, we visualize loads across different datasets.

3.2 Motivation – the Straggler Effect

Under the expert parallelism scenario, where the number of assigned tokens dictates the processing time of each expert, high-load experts become the bottleneck for overall latency within an MoE layer. Specifically, low-load experts remain idle while waiting for high-load experts to complete, leading to synchronization delays. Therefore, the latency of an MoE layer is given by:

$$L \propto \max(\{N_i\}_{i=1}^n), \quad (4)$$

where N_i represents the number of tokens assigned to the i -th expert, with the total token allocation satisfying $\sum_{i=1}^n N_i = tk$. According to Eq. 4, the latency follows the **Straggler Effect: the most burdened experts dictate the overall latency of the MoE layer**. In the worst case, all tokens are assigned to the same group of experts, underutilizing the parallel processing capability of MoE. Conversely, distributing tokens evenly across experts maximizes computational efficiency and fully leverages the parallelism of multiple experts. With the bounds of the ideal and worst cases, the range of the highest load is given by:

$$\max(\{N_i\}_{i=1}^n) \in [\bar{N}, \frac{n\bar{N}}{k}]. \quad (5)$$

However, existing MoE models often adopt a dropless strategy during inference, which fails to address token imbalance and can lead to significantly increased latency.

Given that the imbalance stems from excessively high- and low-load experts, we address this issue by exploring the following questions: (1) For **high-load experts**, are there redundant tokens that can be dropped without causing significant performance degradation? (2) For **low-load experts** that must wait for high-load experts to complete forward passes, is there an opportunity to enhance their utilization and improve performance without incurring substantial additional cost?

4 Methodology

Token Drop Regulates the Latency of High-Load Experts To address the question about overloaded experts, we first regulate their maximum utilization. Specifically, we introduce expert capacity to control token allocation. Given a capacity factor γ , the maximum number of tokens assigned to each expert (i.e., expert capacity) is defined as:

$$C = \gamma \bar{N}. \quad (6)$$

A higher γ allows more tokens to be retained, but experts handling excessive tokens may introduce latency. Conversely, a lower γ enforces stricter capacity limits, reducing latency by discarding more tokens, but at the risk of performance degradation. With the involvement of expert capacity γ , we constrain the upper bound of latency as follows:

$$\max(\{N_i\}_{i=1}^n) = \begin{cases} \gamma \bar{N} & \gamma < 1 \\ \text{within } [\bar{N}, \gamma \bar{N}] & \gamma \geq 1 \end{cases}, \quad (7)$$

where γ is typically much smaller than $\frac{n}{k}$. This constraint ensures that no expert exceeds the specified capacity limit, effectively mitigating severe load imbalances and reducing latency. Note that tokens are distributed across devices under expert and data parallelism. To avoid additional communication overhead, we apply capacity constraints to tokens within each local device, similar to the constraints used during training [14]. This ensures that all devices respect the limits, maintaining strict control over token flow to the experts.

Specifically, when a capacity constraint is imposed on each expert, experts must evaluate the volume of assigned tokens before execution. For experts with a load below the predefined capacity, there is no difference between capacity-constrained inference and traditional inference. However, when the load exceeds the capacity, experts must discard excess tokens to adhere to the constraint. To address this, we introduce a scoring function \mathcal{S} to evaluate each token:

$$\mathcal{S}(\mathbf{x}) = \begin{bmatrix} s_{11} & s_{12} & \dots & s_{1n} \\ s_{21} & s_{22} & \dots & s_{2n} \\ \vdots & \vdots & \vdots & \vdots \\ s_{t1} & s_{t2} & \dots & s_{tn} \end{bmatrix}, \quad (8)$$

where s_{ij} denotes the importance score of the mapping from the i -th token to the j -th expert. With this score, each overflowed expert selectively discards those with lower scores. Let \mathcal{J} be the set of overflowed experts:

$$\tau_{\mathcal{J}} = \text{KthValue}(\mathcal{S}_{\mathcal{J}}, C), \quad (9)$$

where $\tau_{\mathcal{J}}$ represents the thresholds, i.e., C -th highest value in $\mathcal{S}_{\mathcal{J}}$, serving as a threshold to filter out excess tokens:

$$T_{\mathcal{J}} \leftarrow \{(t, j) \mid t \in [1, \dots, N], j \in \mathcal{J}, \mathcal{S}[t, j] \geq \tau_{\mathcal{J}}[j]\} \quad (10)$$

$$\mathcal{S}_{\mathcal{J}} \leftarrow \mathcal{S}_{\mathcal{J}} \odot M_{\mathcal{J}}, \text{ where } M_{\mathcal{J}} \leftarrow \mathbb{1}[\mathcal{S}_{\mathcal{J}} \geq \tau_{\mathcal{J}}], \quad (11)$$

where $T_{\mathcal{J}}$ denotes the token indices retained by the experts indexed in \mathcal{J} . The scores of rejected tokens are masked to prevent them from being routed to their corresponding overflowed experts.

Regarding the specific scoring function, we explore multiple metrics and summarize them as follows:

Order: Discarding later tokens once earlier tokens have filled the expert capacity. This strategy was first introduced in Switch-Transformer [14] during training, and we extend it to the inference phase.

Reverse Order: Instead of discarding later tokens, this approach removes earlier tokens to comply with the expert capacity constraint.

Random: Dropping Excess tokens randomly to meet the predefined expert capacity constraints.

Score: Using the gating score $G(x)$ as an importance indicator and discarding tokens.

Among these metrics, “Order” and “Reverse Order” are unstable, as shuffling sequences within a batch may result in different tokens being dropped [17]. “Random” assumes all tokens have an equal probability of being dropped. In contrast, “Score” is stable, unaffected by sequence order within a batch. Notably, there is virtually no additional computational overhead associated with calculating these metrics, and the dropping operation incurs minimal cost compared to the intensive computations performed by the experts.

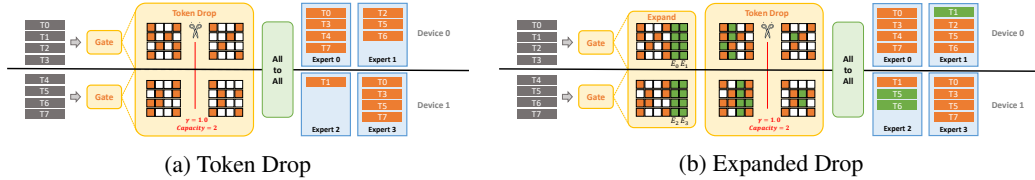


Figure 3: **Illustration of Capacity-Aware Token Drop (a) and Expanded Drop (b).** Both methods first select experts based on gating scores. In Token Drop, tokens exceeding the local device capacity are discarded prior to All-to-All communication. Expanded Drop enhances expert utilization by allowing each token to consider additional m candidate experts on the same device while still enforcing strict local capacity constraints.

Expanded Drop Enhances the Utilization of Low-load Experts Token Drop exclusively targets overloaded experts by discarding overflowed tokens that exceed expert capacity but does not address the underutilization of low-load experts. Next, we introduce Expanded Drop to ensure a more balanced token-to-expert allocation.

A naive approach to rerouting under-selected tokens is to mask the mapping scores of overflowed experts and then reselect experts for these tokens. However, the reselection may still result in overflows, necessitating multiple rounds of selection and dropping, which increases latency. Moreover, the repeated selection and dropping substantially raise the cost of token-to-expert mapping.

Expanded Drop adopts a simple yet effective strategy: for each token, it selects additional candidate experts. Given m experts deployed on a single GPU, a token not only selects the top- k experts based on gating scores, but also includes m local experts (e.g., 8 experts per device under 8-way expert parallelism across 8 GPUs for a total of 64 experts) for substitution if the initially selected experts are overflowed. As a result, each token may select up to $m + k$ experts. The final selection is then refined as experts drop tokens as needed to satisfy capacity constraints. This makes no change in the token assignments in experts that are overflowed by the top- k experts. Meanwhile, for under-utilized experts, the expanded top- $k + m$ candidate pool increases the likelihood of receiving additional

tokens. After $\text{top-}k + m$ selection and dropping, there might exist tokens that select more than k experts. Through empirical analysis (Appendix D), we choose not to enforce a constraint that limits each token to selecting at most k experts, thereby removing the need to explicitly retain the top- k experts at the end.

Notably, the extra cost of token routing is minimal; the only difference lies in the negligible cost in the concatenation of the gating scores from either the top- k or m experts on the local device. Moreover, processing expanded tokens within local device eliminates inter-device communication.

5 Experiments

In this section, we conduct experiments under capacity-aware inference for MoE, with deployment details provided in Appendix A.

5.1 Token Drop for High-load Experts

Table 1: **Performance comparison across different capacity factors and selection metrics** (i.e., Order, Reverse Order, Random, and Score). The baseline operates without capacity constraints, represented as $+\infty$. We report the average performance over multiple random seeds.

Method	γ	OBQA	PIQA	RTE	WinoGrande	BoolQ	ARC-C	HellaSwag	MMLU	Avg.
Baseline	$+\infty$	45.6	80.1	53.7	71.2	74.7	54.5	79.4	52.5	64.0
Order	2.0	42.0	71.5	53.1	71.2	74.2	49.5	76.6	48.4	60.8
Reverse Order		41.8	71.8	52.7	71.0	73.9	49.4	76.4	49.2	60.8
Random		41.2	75.2	52.7	71.0	74.1	50.1	76.8	49.4	61.3
Score		45.0	80.1	54.5	71.5	74.6	54.9	79.3	51.8	64.0
Order	1.5	38.8	67.1	48.7	68.5	73.3	46.3	54.0	43.7	55.1
Reverse Order		40.2	67.3	52.7	70.1	72.7	45.5	54.4	45.2	56.0
Random		39.6	72.1	53.8	68.3	73.8	45.8	74.2	45.2	59.1
Score		44.8	77.5	55.2	70.8	74.3	53.4	78.6	50.0	63.1
Order	1.0	36.0	60.2	52.2	62.6	69.6	38.7	58.0	36.9	51.8
Reverse Order		36.2	59.5	50.5	63.3	69.4	39.4	58.7	38.7	52.0
Random		34.0	63.1	53.2	60.8	70.2	40.5	66.9	35.7	53.1
Score		41.6	76.0	53.4	69.9	73.2	50.4	77.1	47.8	61.1

Investigation on Token Drop Metrics To assess the effectiveness of different metrics in regulating token load to the target capacity, we compare various approaches on OLMoE by discarding excess tokens and applying a range of capacity factors. As shown in Table 1, varying the dropping metrics impacts performance at different levels. With higher capacities, the model maintains comparable performance even when using naive selection methods like “Random”. However, as the capacity factor decreases, performance degradation becomes more pronounced, particularly for “Order”, “Reverse Order”, and “Random”. Notably, “Score” consistently outperforms other methods by a large margin, demonstrating the effectiveness of leveraging gating scores as an importance measure. Consequently, we adopt “Score” as the default metric.

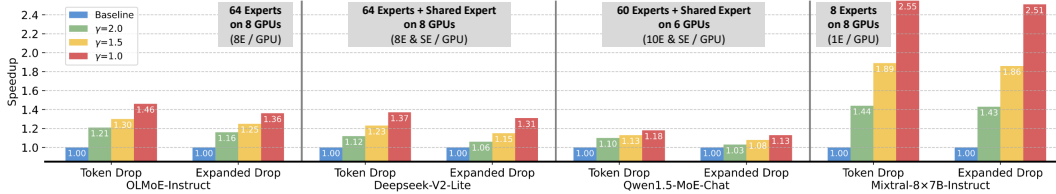


Figure 4: Speedup of a single MoE layer compared to the baseline without capacity constraints, achieved through two capacity-aware inference methods: Token Drop and Expanded Drop.

Efficiency Gains from Capacity-Constrained Inference We next explore the efficiency improvements achieved by imposing expert capacity. Specifically, we employ distributed inference using eight H20 GPUs, utilizing an 8-way Data Parallelism (DP) and 8-way Expert Parallelism (EP) strategy through the Megatron-LM framework [36]. Notably, in Mixtral-8×7B-Instruct model, each GPU

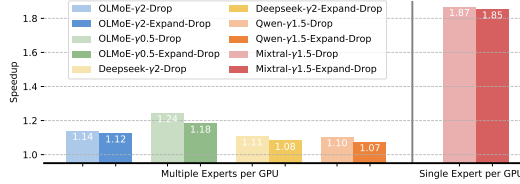


Figure 5: End-to-End Model Speedup

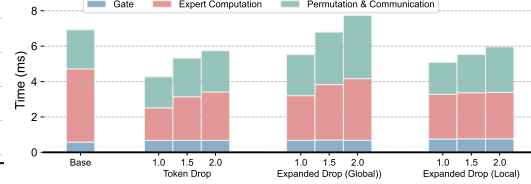


Figure 6: Breakdown Analysis on OLMoE

hosts a single expert, whereas, in models like OLMoE-Instruct, multiple experts must be deployed on a single GPU (e.g., eight experts per GPU) due to GPU resource constraints.

As illustrated in Figure 4, imposing constraints on expert capacity through Token Drop and Expanded Drop, considerably accelerates inference across the four tested MoE models, in comparison to the baseline model without capacity limitations. The enhanced efficiency of each MoE layer (Figure 4) contributes to faster end-to-end model inference (Figure 5). Moreover, as the capacity factor γ decreases, capacity-aware inference methods achieve significantly greater acceleration.

Notably, the efficacy of acceleration is influenced by the numerical relationship between the total experts and the engaged GPUs in Expert Parallelism. As illustrated in Figure 5, for Mixtral-8 \times 7B-Instruct, deploying a single expert per GPU maximizes the effectiveness of capacity-aware inference. In this configuration, Token Drop and Expanded Drop achieve end-to-end model speedups of $1.87 \times$ and $1.85 \times$, respectively, with $\gamma = 1.5$. Conversely, deploying a greater number of experts on a single GPU results in more modest acceleration gains, as evidenced by the “8E/GPU” (OLMoE-Instruct and Deepseek-V2-Lite) the “10E/GPU” (Qwen1.5-MoE-Chat) in Figure 4 and Figure 5. This is because the aggregated load from multiple experts diminishes the proportion of reduced load, which is achieved by limiting the straggler expert. Therefore, it is anticipated that allocating more GPUs for expert distribution, thereby reducing the number of experts per GPU, would enhance the acceleration effect of capacity-aware inference.

The breakdown analysis presented in Figure 6 demonstrates that our proposed capacity-aware inference methods substantially reduce the duration of expert computation, permutation and communication, while preserving a comparable cost for gate processing. Notably, the duration of permutation and communication increases when tokens are expanded across a range of global experts. This is due to the increased communication workload required to transmit expanded global tokens across various GPU devices. Consequently, these results underscore the necessity of restricting the expanded tokens to be processed by local experts.

Mitigating the Straggler Effect with Minimal Token Discarding

Given that expert capacity enforces MoE layers to discard overflowed tokens, we next establish the relationship between expert capacity and the corresponding number of dropped tokens. For a capacity factor γ , the total proportion of dropped tokens is given by:

$$DT = \frac{\sum_{i=1}^n \text{ReLU}(N_i - \gamma \bar{N})}{\sum_{i=1}^n N_i}, \quad (12)$$

where $\text{ReLU}(N_i - \gamma \bar{N})$ represent the number of dropped tokens for the i -th expert.

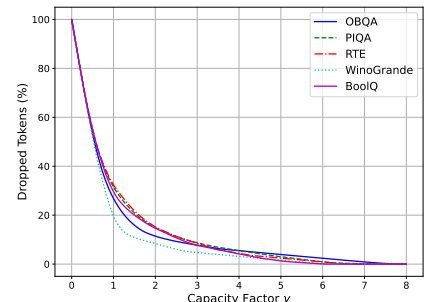


Figure 7: Analysis of dropped tokens with respect to capacity factors.

Figure 7 visualizes the number of dropped tokens across different capacity factors for various test datasets, with a more detailed illustration provided in Appendix F. Although the most overloaded expert receives much more tokens than the expected number of tokens \bar{N} , regulating the maximum capacity has a limited impact on the overall number of accommodated tokens, thereby maintaining competitive performance even after discarding overflow tokens. Moreover, dropping a small proportion of overflowed tokens can significantly reduce the latency caused by overloaded experts (e.g., dropping 12% of overloaded tokens promotes the inference speed by 85% in Mixtral-8 \times 7B-Instruct), highlighting the efficacy of capacity-aware inference in improving both performance and efficiency.

Table 2: **Comparison of Expert Drop, Token Drop and Expanded Drop.** The capacity factor γ is set to 2.0 for OLMoE and DeepSeek-V2-Lite, and 1.5 for Qwen1.5-MoE-Chat and Mixtral-8×7B-Instruct. For Expert Drop, each forward pass skips one out of eight experts for Mixtral-8×7B-Instruct, and the bottom 10% of lowest load experts for other models.

Model	Method	OBQA	PIQA	RTE	WinoGrande	BoolQ	ARC-C	HellaSwag	MMLU	GSM8K	Avg.
OLMoE-Instruct	Baseline	47.6	80.2	67.9	69.9	80.7	57.0	80.6	52.8	35.1	63.5
	Expert Drop	44.6	76.9	64.0	67.6	78.2	54.4	77.0	50.6	31.6	60.5
	Token Drop	47.8	77.9	64.6	69.2	80.0	57.2	79.7	51.5	32.4	62.3
	Expanded Drop	47.2	79.4	66.3	70.5	80.9	57.1	80.3	52.3	34.4	63.2
Qwen1.5-MoE-Chat	Baseline	42.4	79.9	72.9	70.0	81.3	54.1	80.4	59.8	52.0	65.9
	Expert Drop	41.4	78.7	71.2	68.6	80.6	52.9	79.1	58.1	49.4	64.4
	Token Drop	40.4	78.8	72.6	69.1	80.9	53.0	80.0	59.3	51.9	65.1
	Expanded Drop	43.4	79.1	72.6	69.6	81.1	53.4	80.3	59.3	52.1	65.6
DeepSeek-V2-Lite-Chat	Baseline	45.4	81.4	72.6	75.5	82.9	61.0	81.5	57.3	66.4	69.3
	Expert Drop	41.8	77.6	71.9	72.5	81.6	57.1	75.5	53.3	56.0	65.3
	Token Drop	45.2	78.3	72.6	74.0	83.2	59.3	80.9	57.3	62.7	68.2
	Expanded Drop	45.4	79.4	73.3	75.4	83.2	60.4	81.5	57.2	64.1	68.9
Mixtral-8×7B-Instruct	Baseline	47.4	84.8	71.8	82.5	88.5	71.7	87.5	70.2	64.2	74.3
	Expert Drop	46.8	83.2	70.1	81.3	87.6	67.1	85.6	66.2	62.3	72.2
	Token Drop	46.4	83.3	71.7	82.2	88.3	71.2	87.4	69.1	64.7	73.8
	Expanded Drop	47.8	85.0	71.8	83.0	88.6	71.5	87.6	70.2	64.6	74.5

5.2 Expanded Drop to Low-load Experts

Besides the experts overloaded with tokens, some low-load experts receive only a few tokens, raising important questions: Are these low-load experts redundant and removable, or should they be leveraged to balance token allocation? Recent works [29, 19] remove less important experts to improve efficiency, while our proposed Expanded Drop increases their utilization by redistributing tokens for a more balanced assignment. Next, we investigate the significance of low-load experts and validate the effectiveness of Expanded Drop.

The Critical Role of Low-Load Experts To explore the impact of low-load experts, we further compare dropping tokens (i.e., Token Drop) with skipping experts (i.e., Expert Drop). For Expert Drop, we adopt a conservative strategy that dynamically skips the 10% of experts with the lowest token loads. Notably, the proportion of tokens removed in Expert Drop is significantly lower than in Token Drop (2% in Expert Drop vs. 12% in Token Drop on OLMoE-Instruct).

Despite this, as shown in Table 2, Expert Drop experiences significant performance degradation and is outperformed by Token Drop by a large margin. Moreover, due to the small proportion of tokens assigned to low-load experts, removing these experts provides only marginal improvements in inference speed (less than a 5% speedup). These findings indicate that retaining low-load experts better preserves the performance of MoE models.

Effectiveness of Expanded Drop We examine the effectiveness of utilizing low-load experts by Expanded Drop instead of simply discarding these tokens to meet the target capacity. Comparing Expanded Drop with Token Drop, redistributing excess tokens to low-load experts enhances performance, yielding a 0.9% improvement in the average performance of Qwen1.5-MoE-Chat. Furthermore, considering the performance degradation observed in Expert Drop, our findings highlight the crucial role of low-load experts in maintaining model effectiveness.

Expanded Drop overselects experts for each token to expand the selection scope to prompt a more balanced token-expert assignments. As shown in Figure 8, increasing the overselection ratio m allows tokens to consider more candidate experts after being dropped from overflowed ones, thereby improving low-load expert utilization and balancing the expert load.

5.3 Extension to Multi-modal Mixture of Experts

In addition to applying capacity-aware inference to MoE models for language tasks, we also explore its effectiveness in multi-modal MoE settings. Specifically, we evaluate the OLMoE based MolmoE [12], across multi-modal benchmarks, including MME [15], MMBench [28], and SEED-Bench [27].

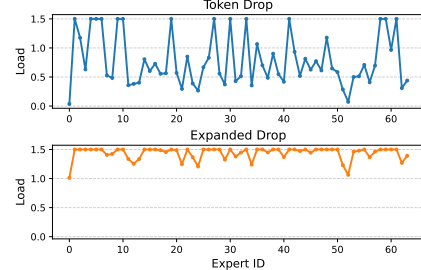


Figure 8: Normalized expert load after Token Drop and Expanded Drop, with the capacity ratio set to $\gamma = 1.5$.

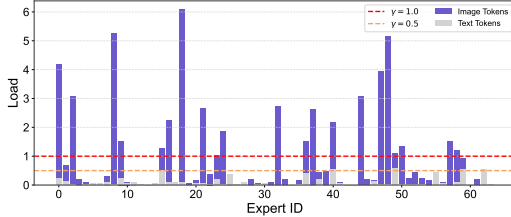


Figure 9: Multi-modal token assignments across different experts.

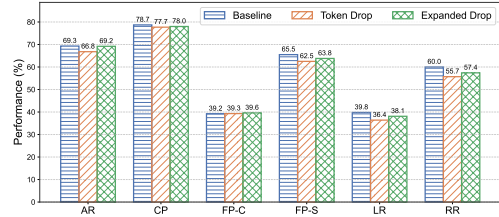


Figure 10: Comparison on MMBench across six multimodal capabilities in Appendix B.

Given that the input sequence contains tokens from multiple modalities, we first investigate different token dropping strategies. Specifically, we first treat all tokens equally and drops those with the lowest scores (“Uniform”). Beyond this, considering the redundancy often found in image tokens, we also experiment with a strategy that prioritizes dropping image tokens before selectively removing text tokens (“Image First”). For comparison, we also consider drop text tokens first (“Text First”). As shown in Table 3, on the MME benchmark, this image-first strategy yields improved performance, highlighting the benefit of prioritizing dropping image tokens for the load balance in multi-modal MoE models.

Given the redundancy of image tokens and their large proportion in multi-modal tasks, we further investigate more aggressive capacity factors for Token Drop and Expanded Drop using the “Image First” strategy. Figure 10 demonstrates the effectiveness of Capacity-Aware Inference under low capacity constraints (i.e., $\gamma = 0.5$). This is largely due to the high redundancy in image tokens [4], which allows a higher dropping ratio without significantly affecting performance. Meanwhile, the dominance of image tokens enables the use of very low capacity factors without significantly affecting text token retention, as illustrated in Figure 9. Therefore, dropping image tokens at higher ratios leads to more balanced token assignments and substantially improved inference efficiency.

5.4 Ablation Study

Model-Specific Imbalanced Property We explore the imbalance property in various models, such as OLMoE, DeepSeek, Qwen and Mixtral, which differ in both architectures (e.g., depth and width) and training strategies (e.g., training from scratch [31, 10] vs. training after upcycling [22, 39]).

On the one hand, our findings in Appendix E reveal different training strategies result in significantly varying levels of imbalance. Specifically, MoE models trained from scratch exhibit a much higher degree of imbalance. For instance, OLMoE and DeepSeek-V2-Lite experience peak expert-wise token allocations exceeding $5N$, whereas Qwen1.5-MoE and Mixtral are upcycled from dense language models, maintain a more balanced distribution, with peak expert-wise allocations staying below $3N$. This is because upcycling initializes all experts with identical parameters [24], reducing divergence and promoting balanced training in the early stages.

On the other hand, despite the widespread use of auxiliary balance loss in MoE training, it does not guarantee balanced token assignments across experts, as token distribution still varies significantly during inference on test data. This necessitates integrating expert capacity into the inference process.

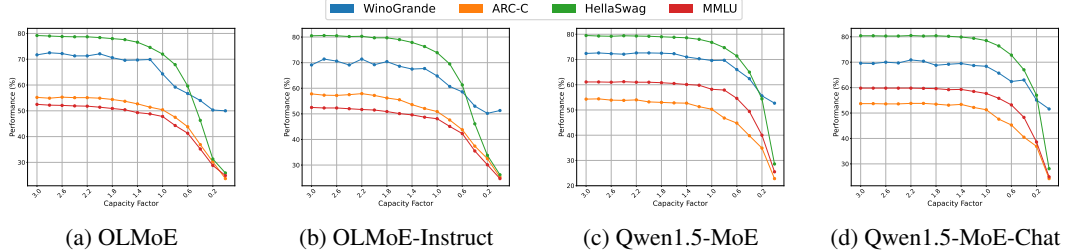


Figure 11: Performance change as capacity factors decrease from 3.0 to 0.0.

Table 3: **Capacity-aware inference for Multi-modality MoE models** under different routing strategies. “Percep.” and “Cognit.” denote Perception and Cognition, respectively. γ is set to 1.0.

Method	Strategy	Percep.	Cognit.
Baseline	–	1358.1	269.6
Token Drop	Uniform	1248.4	245.4
		1307.6	273.6
Expanded Drop	Text First	1114.2	214.4
	Image First	1163.6	241.3
Token Drop	Image First	1346.5	288.9
	Expanded Drop	1362.1	297.1

Capacity Factor Beyond the specific capacity values presented in Table 1, we further investigate a wide range of capacity factors in Figure 11, spanning from 0.0 to 3.0. We exclude values exceeding 3.0, as their performance closely aligns with capacity-agnostic scenarios. By analyzing the performance changes when decreasing the capacity factor, we find that setting γ to 1.5 is sufficient to maintain performance comparable to the original models. However, maintaining performance becomes challenging under excessively low capacity factors, as high-load experts are forced to drop a significant number of tokens.

6 Conclusion

In this paper, we identify the issue of imbalanced token-to-expert assignment in Mixture of Experts (MoE) models and introduce the Straggler Effect during inference, where high-load experts become efficiency bottlenecks and dictate overall latency. To address this problem, we propose Capacity-Aware Token Drop, which mitigates expert overload by enforcing strict capacity constraints. Additionally, to better utilize underloaded experts, we present Capacity-Aware Expanded Drop, which allows tokens to select additional experts on the same device while still respecting capacity limits, thereby improving expert utilization. Our findings and proposed methods offer valuable insights and effective strategies for improving MoE inference efficiency.

References

- [1] Winogrande: An adversarial winograd schema challenge at scale. 2019.
- [2] Yonatan Bisk, Rowan Zellers, Ronan Le Bras, Jianfeng Gao, and Yejin Choi. Piqa: Reasoning about physical commonsense in natural language, 2019.
- [3] Weilin Cai, Juyong Jiang, Fan Wang, Jing Tang, Sunghun Kim, and Jiayi Huang. A survey on mixture of experts, 2024. URL <https://arxiv.org/abs/2407.06204>.
- [4] Liang Chen, Haozhe Zhao, Tianyu Liu, Shuai Bai, Junyang Lin, Chang Zhou, and Baobao Chang. An image is worth 1/2 tokens after layer 2: Plug-and-play inference acceleration for large vision-language models, 2024.
- [5] Zixiang Chen, Yihe Deng, Yue Wu, Quanquan Gu, and Yuanzhi Li. Towards understanding the mixture-of-experts layer in deep learning. In Alice H. Oh, Alekh Agarwal, Danielle Belgrave, and Kyunghyun Cho, editors, *Advances in Neural Information Processing Systems*, 2022. URL <https://openreview.net/forum?id=MaYzugDmQV>.
- [6] Christopher Clark, Kenton Lee, Ming-Wei Chang, Tom Kwiatkowski, Michael Collins, and Kristina Toutanova. Boolq: Exploring the surprising difficulty of natural yes/no questions, 2019.
- [7] Peter Clark, Isaac Cowhey, Oren Etzioni, Tushar Khot, Ashish Sabharwal, Carissa Schoenick, and Oyvind Tafjord. Think you have solved question answering? try arc, the ai2 reasoning challenge, 2018.
- [8] Karl Cobbe, Vineet Kosaraju, Mohammad Bavarian, Mark Chen, Heewoo Jun, Lukasz Kaiser, Matthias Plappert, Jerry Tworek, Jacob Hilton, Reiichiro Nakano, Christopher Hesse, and John Schulman. Training verifiers to solve math word problems. *arXiv preprint arXiv:2110.14168*, 2021.
- [9] Damai Dai, Chengqi Deng, Chenggang Zhao, RX Xu, Huazuo Gao, Deli Chen, Jiashi Li, Wangding Zeng, Xingkai Yu, Y Wu, et al. Deepseekmoe: Towards ultimate expert specialization in mixture-of-experts language models. *arXiv preprint arXiv:2401.06066*, 2024.
- [10] DeepSeek-AI, Aixin Liu, Bei Feng, Bin Wang, Bingxuan Wang, Bo Liu, Chenggang Zhao, Chengqi Deng, Chong Ruan, Damai Dai, Daya Guo, Dejian Yang, Deli Chen, Dongjie Ji, Erhang Li, Fangyun Lin, Fuli Luo, Guangbo Hao, Guanting Chen, Guowei Li, H. Zhang, Hanwei Xu, Hao Yang, Haowei Zhang, Honghui Ding, Huajian Xin, Huazuo Gao, Hui Li, Hui Qu, J. L. Cai, Jian Liang, Jianzhong Guo, Jiaqi Ni, Jiashi Li, Jin Chen, Jingyang Yuan, Junjie Qiu, Junxiao Song, Kai Dong, Kaige Gao, Kang Guan, Lean Wang, Lecong Zhang,

Lei Xu, Leyi Xia, Liang Zhao, Liyue Zhang, Meng Li, Miaojun Wang, Mingchuan Zhang, Minghua Zhang, Minghui Tang, Mingming Li, Ning Tian, Panpan Huang, Peiyi Wang, Peng Zhang, Qihao Zhu, Qinyu Chen, Qiushi Du, R. J. Chen, R. L. Jin, Ruiqi Ge, Ruizhe Pan, Runxin Xu, Ruyi Chen, S. S. Li, Shanghao Lu, Shangyan Zhou, Shanhua Chen, Shaoqing Wu, Shengfeng Ye, Shirong Ma, Shiyu Wang, Shuang Zhou, Shuiping Yu, Shunfeng Zhou, Size Zheng, T. Wang, Tian Pei, Tian Yuan, Tianyu Sun, W. L. Xiao, Wangding Zeng, Wei An, Wen Liu, Wenfeng Liang, Wenjun Gao, Wentao Zhang, X. Q. Li, Xiangyue Jin, Xianzu Wang, Xiao Bi, Xiaodong Liu, Xiaohan Wang, Xiaojin Shen, Xiaokang Chen, Xiaosha Chen, Xiaotao Nie, Xiaowen Sun, Xiaoxiang Wang, Xin Liu, Xin Xie, Xingkai Yu, Xinnan Song, Xinyi Zhou, Xinyu Yang, Xuan Lu, Xuecheng Su, Y. Wu, Y. K. Li, Y. X. Wei, Y. X. Zhu, Yanhong Xu, Yanping Huang, Yao Li, Yao Zhao, Yaofeng Sun, Yaohui Li, Yaohui Wang, Yi Zheng, Yichao Zhang, Yiliang Xiong, Yilong Zhao, Ying He, Ying Tang, Yishi Piao, Yixin Dong, Yixuan Tan, Yiyuan Liu, Yongji Wang, Yongqiang Guo, Yuchen Zhu, Yuduan Wang, Yuheng Zou, Yukun Zha, Yunxian Ma, Yuting Yan, Yuxiang You, Yuxuan Liu, Z. Z. Ren, Zehui Ren, Zhangli Sha, Zhe Fu, Zhen Huang, Zhen Zhang, Zhenda Xie, Zhewen Hao, Zhihong Shao, Zhiniu Wen, Zhipeng Xu, Zhongyu Zhang, Zhuoshu Li, Zihan Wang, Zihui Gu, Zilin Li, and Ziwei Xie. Deepseek-v2: A strong, economical, and efficient mixture-of-experts language model, 2024. URL <https://arxiv.org/abs/2405.04434>.

[11] DeepSeek-AI, Aixin Liu, Bei Feng, Bing Xue, Bingxuan Wang, Bochao Wu, Chengda Lu, Chenggang Zhao, Chengqi Deng, Chenyu Zhang, Chong Ruan, Damai Dai, Daya Guo, Dejian Yang, Deli Chen, Dongjie Ji, Erhang Li, Fangyun Lin, Fucong Dai, Fuli Luo, Guangbo Hao, Guanting Chen, Guowei Li, H. Zhang, Han Bao, Hanwei Xu, Haocheng Wang, Haowei Zhang, Honghui Ding, Huajian Xin, Huazuo Gao, Hui Li, Hui Qu, J. L. Cai, Jian Liang, Jianzhong Guo, Jiaqi Ni, Jiashi Li, Jiawei Wang, Jin Chen, Jingchang Chen, Jingyang Yuan, Junjie Qiu, Junlong Li, Junxiao Song, Kai Dong, Kai Hu, Kaige Gao, Kang Guan, Kexin Huang, Kuai Yu, Lean Wang, Lecong Zhang, Lei Xu, Leyi Xia, Liang Zhao, Litong Wang, Liyue Zhang, Meng Li, Miaojun Wang, Mingchuan Zhang, Minghua Zhang, Minghui Tang, Mingming Li, Ning Tian, Panpan Huang, Peiyi Wang, Peng Zhang, Qiancheng Wang, Qihao Zhu, Qinyu Chen, Qiushi Du, R. J. Chen, R. L. Jin, Ruiqi Ge, Ruisong Zhang, Ruizhe Pan, Runji Wang, Runxin Xu, Ruoyu Zhang, Ruyi Chen, S. S. Li, Shanghao Lu, Shangyan Zhou, Shanhua Chen, Shaoqing Wu, Shengfeng Ye, Shengfeng Ye, Shirong Ma, Shiyu Wang, Shuang Zhou, Shuiping Yu, Shunfeng Zhou, Shuting Pan, T. Wang, Tao Yun, Tian Pei, Tianyu Sun, W. L. Xiao, Wangding Zeng, Wanjia Zhao, Wei An, Wen Liu, Wenfeng Liang, Wenjun Gao, Wenqin Yu, Wentao Zhang, X. Q. Li, Xiangyue Jin, Xianzu Wang, Xiao Bi, Xiaodong Liu, Xiaohan Wang, Xiaojin Shen, Xiaokang Chen, Xiaokang Zhang, Xiaosha Chen, Xiaotao Nie, Xiaowen Sun, Xiaoxiang Wang, Xin Cheng, Xin Liu, Xin Xie, Xingchao Liu, Xingkai Yu, Xinnan Song, Xinxia Shan, Xinyi Zhou, Xinyu Yang, Xinyuan Li, Xuecheng Su, Xuheng Lin, Y. K. Li, Y. Q. Wang, Y. X. Wei, Y. X. Zhu, Yang Zhang, Yanhong Xu, Yanhong Xu, Yanping Huang, Yao Li, Yao Zhao, Yaofeng Sun, Yaohui Li, Yaohui Wang, Yi Yu, Yi Zheng, Yichao Zhang, Yifan Shi, Yiliang Xiong, Ying He, Ying Tang, Yishi Piao, Yisong Wang, Yixuan Tan, Yiyang Ma, Yiyuan Liu, Yongqiang Guo, Yu Wu, Yuan Ou, Yuchen Zhu, Yuduan Wang, Yue Gong, Yuheng Zou, Yujia He, Yukun Zha, Yunfan Xiong, Yunxian Ma, Yuting Yan, Yuxiang Luo, Yuxiang You, Yuxuan Liu, Yuyang Zhou, Z. F. Wu, Z. Z. Ren, Zehui Ren, Zhangli Sha, Zhe Fu, Zhean Xu, Zhen Huang, Zhen Zhang, Zhenda Xie, Zhengyan Zhang, Zhewen Hao, Zhibin Gou, Zhicheng Ma, Zhihong Yan, Zhihong Shao, Zhipeng Xu, Zhiyu Wu, Zhongyu Zhang, Zhuoshu Li, Zihui Gu, Zijia Zhu, Zijun Liu, Zilin Li, Ziwei Xie, Ziyang Song, Ziyi Gao, and Zizheng Pan. Deepseek-v3 technical report, 2024. URL <https://arxiv.org/abs/2412.19437>.

[12] Matt Deitke, Christopher Clark, Sangho Lee, Rohun Tripathi, Yue Yang, Jae Sung Park, Mohammadreza Salehi, Niklas Muennighoff, Kyle Lo, Luca Soldaini, Jiasen Lu, Taira Anderson, Erin Bransom, Kiana Ehsani, Huong Ngo, YenSung Chen, Ajay Patel, Mark Yatskar, Chris Callison-Burch, Andrew Head, Rose Hendrix, Favyen Bastani, Eli VanderBilt, Nathan Lambert, Yvonne Chou, Arnavi Chheda, Jenna Sparks, Sam Skjonsberg, Michael Schmitz, Aaron Sarnat, Byron Bischoff, Pete Walsh, Chris Newell, Piper Wolters, Tanmay Gupta, Kuo-Hao Zeng, Jon Borchardt, Dirk Groeneveld, Jen Dumas, Crystal Nam, Sophie Lebrecht, Caitlin Wittlif, Carissa Schoenick, Oscar Michel, Ranjay Krishna, Luca Weihs, Noah A. Smith, Hannaneh Hajishirzi, Ross Girshick, Ali Farhadi, and Aniruddha Kembhavi. Molmo and pixmo: Open weights and open data for state-of-the-art multimodal models. *arXiv preprint arXiv:2409.17146*, 2024.

[13] Nan Du, Yanping Huang, Andrew M Dai, Simon Tong, Dmitry Lepikhin, Yuanzhong Xu, Maxim Krikun, Yanqi Zhou, Adams Wei Yu, Orhan Firat, et al. Glam: Efficient scaling of language models with mixture-of-experts. In *International Conference on Machine Learning*, pages 5547–5569. PMLR, 2022.

[14] William Fedus, Barret Zoph, and Noam Shazeer. Switch transformers: Scaling to trillion parameter models with simple and efficient sparsity. *Journal of Machine Learning Research*, 23(120):1–39, 2022.

[15] Chaoyou Fu, Peixian Chen, Yunhang Shen, Yulei Qin, Mengdan Zhang, Xu Lin, Zhenyu Qiu, Wei Lin, Jinrui Yang, Xiawu Zheng, Ke Li, Xing Sun, and Rongrong Ji. Mme: A comprehensive evaluation benchmark for multimodal large language models. *ArXiv*, abs/2306.13394, 2023. URL <https://api.semanticscholar.org/CorpusID:259243928>.

[16] Leo Gao, Jonathan Tow, Baber Abbasi, Stella Biderman, Sid Black, Anthony DiPofi, Charles Foster, Laurence Golding, Jeffrey Hsu, Alain Le Noac'h, Haonan Li, Kyle McDonell, Niklas Muennighoff, Chris Ociepa, Jason Phang, Laria Reynolds, Hailey Schoelkopf, Aviya Skowron, Lintang Sutawika, Eric Tang, Anish Thite, Ben Wang, Kevin Wang, and Andy Zou. A framework for few-shot language model evaluation, 12 2023. URL <https://zenodo.org/records/10256836>.

[17] Jamie Hayes, Ilia Shumailov, and Itay Yona. Buffer overflow in mixture of experts. In *Neurips Safe Generative AI Workshop 2024*, 2024. URL <https://openreview.net/forum?id=SKWidEjUgU>.

[18] Shuai He, Liang Ding, Daize Dong, Boan Liu, Fuqiang Yu, and Dacheng Tao. PAD-net: An efficient framework for dynamic networks. In Anna Rogers, Jordan Boyd-Graber, and Naoaki Okazaki, editors, *Proceedings of the 61st Annual Meeting of the Association for Computational Linguistics (Volume 1: Long Papers)*, pages 14354–14366, Toronto, Canada, July 2023. Association for Computational Linguistics. doi: 10.18653/v1/2023.acl-long.803. URL <https://aclanthology.org/2023.acl-long.803>.

[19] Shuai He, Daize Dong, Liang Ding, and Ang Li. Demystifying the compression of mixture-of-experts through a unified framework, 2024. URL <https://arxiv.org/abs/2406.02500>.

[20] Dan Hendrycks, Collin Burns, Steven Basart, Andy Zou, Mantas Mazeika, Dawn Song, and Jacob Steinhardt. Measuring massive multitask language understanding, 2021.

[21] Robert A Jacobs, Michael I Jordan, Steven J Nowlan, and Geoffrey E Hinton. Adaptive mixtures of local experts. *Neural computation*, 3(1):79–87, 1991.

[22] Albert Q Jiang, Alexandre Sablayrolles, Antoine Roux, Arthur Mensch, Blanche Savary, Chris Bamford, Devendra Singh Chaplot, Diego de las Casas, Emma Bou Hanna, Florian Bressand, et al. Mixtral of experts. *arXiv preprint arXiv:2401.04088*, 2024.

[23] Michael I Jordan and Robert A Jacobs. Hierarchical mixtures of experts and the em algorithm. *Neural computation*, 6(2):181–214, 1994.

[24] Aran Komatsuzaki, Joan Puigcerver, James Lee-Thorp, Carlos Riquelme Ruiz, Basil Mustafa, Joshua Ainslie, Yi Tay, Mostafa Dehghani, and Neil Houlsby. Sparse upcycling: Training mixture-of-experts from dense checkpoints. In *The Eleventh International Conference on Learning Representations*, 2023. URL <https://openreview.net/forum?id=T5nUQDrM4u>.

[25] Dmitry Lepikhin, HyoukJoong Lee, Yuanzhong Xu, Dehao Chen, Orhan Firat, Yanping Huang, Maxim Krikun, Noam Shazeer, and Zhifeng Chen. Gshard: Scaling giant models with conditional computation and automatic sharding. *arXiv preprint arXiv:2006.16668*, 2020.

[26] Dmitry Lepikhin, HyoukJoong Lee, Yuanzhong Xu, Dehao Chen, Orhan Firat, Yanping Huang, Maxim Krikun, Noam Shazeer, and Zhifeng Chen. {GS}hard: Scaling giant models with conditional computation and automatic sharding. In *International Conference on Learning Representations*, 2021. URL <https://openreview.net/forum?id=qrwe7XHTmYb>.

[27] Bohao Li, Yuying Ge, Yixiao Ge, Guangzhi Wang, Rui Wang, Ruimao Zhang, and Ying Shan. Seed-bench: Benchmarking multimodal large language models. *2024 IEEE/CVF Conference on Computer Vision and Pattern Recognition (CVPR)*, pages 13299–13308, 2024. URL <https://api.semanticscholar.org/CorpusID:271963485>.

[28] Yuanzhan Liu, Haodong Duan, Yuanhan Zhang, Bo Li, Songyang Zhang, Wangbo Zhao, Yike Yuan, Jiaqi Wang, Conghui He, Ziwei Liu, Kai Chen, and Daha Lin. Mmbench: Is your multi-modal model an all-around player? In *European Conference on Computer Vision*, 2023. URL <https://api.semanticscholar.org/CorpusID:259837088>.

[29] Xudong Lu, Qi Liu, Yuhui Xu, Aojun Zhou, Siyuan Huang, Bo Zhang, Junchi Yan, and Hongsheng Li. Not all experts are equal: Efficient expert pruning and skipping for mixture-of-experts large language models, 2024.

[30] Todor Mihaylov, Peter Clark, Tushar Khot, and Ashish Sabharwal. Can a suit of armor conduct electricity? a new dataset for open book question answering, 2018.

[31] Niklas Muennighoff, Luca Soldaini, Dirk Groeneveld, Kyle Lo, Jacob Morrison, Sewon Min, Weijia Shi, Pete Walsh, Oyvind Tafjord, Nathan Lambert, Yuling Gu, Shane Arora, Akshita Bhagia, Dustin Schwenk, David Wadden, Alexander Wettig, Binyuan Hui, Tim Dettmers, Douwe Kiela, Ali Farhadi, Noah A. Smith, Pang Wei Koh, Amanpreet Singh, and Hannaneh Hajishirzi. Olmoe: Open mixture-of-experts language models, 2024. URL <https://arxiv.org/abs/2409.02060>.

[32] OpenAI. Gpt-4 technical report, 2024.

[33] Carlos Riquelme, Joan Puigcerver, Basil Mustafa, Maxim Neumann, Rodolphe Jenatton, André Susano Pinto, Daniel Keysers, and Neil Houlsby. Scaling vision with sparse mixture of experts. *Advances in Neural Information Processing Systems*, 34:8583–8595, 2021.

[34] Noam Shazeer, Azalia Mirhoseini, Krzysztof Maziarz, Andy Davis, Quoc Le, Geoffrey Hinton, and Jeff Dean. Outrageously large neural networks: The sparsely-gated mixture-of-experts layer. *arXiv preprint arXiv:1701.06538*, 2017.

[35] Noam Shazeer, Azalia Mirhoseini, Krzysztof Maziarz, Andy Davis, Quoc Le, Geoffrey Hinton, and Jeff Dean. Outrageously large neural networks: The sparsely-gated mixture-of-experts layer, 2017. URL <https://arxiv.org/abs/1701.06538>.

[36] Mohammad Shoeybi, Mostafa Patwary, Raul Puri, Patrick LeGresley, Jared Casper, and Bryan Catanzaro. Megatron-lm: Training multi-billion parameter language models using model parallelism. *arXiv preprint arXiv:1909.08053*, 2019.

[37] Yixin Song, Zeyu Mi, Haotong Xie, and Haibo Chen. Powerinfer: Fast large language model serving with a consumer-grade gpu, 2023.

[38] Gemini Team. Gemini 1.5: Unlocking multimodal understanding across millions of tokens of context, 2024.

[39] Qwen Team. Qwen1.5-moe: Matching 7b model performance with 1/3 activated parameters", February 2024. URL <https://qwenlm.github.io/blog/qwen-moe/>.

[40] Alex Wang, Amanpreet Singh, Julian Michael, Felix Hill, Omer Levy, and Samuel R. Bowman. GLUE: A multi-task benchmark and analysis platform for natural language understanding. 2019. In the Proceedings of ICLR.

[41] Fuzhao Xue, Zian Zheng, Yao Fu, Jinjie Ni, Zangwei Zheng, Wangchunshu Zhou, and Yang You. Openmoe: An early effort on open mixture-of-experts language models. *arXiv preprint arXiv:2402.01739*, 2024.

[42] Leyang Xue, Yao Fu, Zhan Lu, Luo Mai, and Mahesh Marina. Moe-infinity: Activation-aware expert offloading for efficient moe serving, 2024.

[43] Rowan Zellers, Ari Holtzman, Yonatan Bisk, Ali Farhadi, and Yejin Choi. Hellaswag: Can a machine really finish your sentence?, 2019.

- [44] Yanqi Zhou, Tao Lei, Hanxiao Liu, Nan Du, Yanping Huang, Vincent Y Zhao, Andrew M. Dai, Zhifeng Chen, Quoc V Le, and James Laudon. Mixture-of-experts with expert choice routing. In Alice H. Oh, Alekh Agarwal, Danielle Belgrave, and Kyunghyun Cho, editors, *Advances in Neural Information Processing Systems*, 2022. URL <https://openreview.net/forum?id=jdJo1HIVinI>.
- [45] Tong Zhu, Xiaoye Qu, Daize Dong, Jiacheng Ruan, Jingqi Tong, Conghui He, and Yu Cheng. Llama-moe: Building mixture-of-experts from llama with continual pre-training. *arXiv preprint arXiv:2406.16554*, 2024. URL <https://arxiv.org/abs/2406.16554>.
- [46] Barret Zoph, Irwan Bello, Sameer Kumar, Nan Du, Yanping Huang, Jeff Dean, Noam Shazeer, and William Fedus. St-moe: Designing stable and transferable sparse expert models. *arXiv preprint arXiv:2202.08906*, 2022.

A Implementation Details

Models We mainly focus on lightweight MoE models (less than 20B parameter budget). We conduct experiments on OLMoE [31], Qwen1.5-MoE [39], DeepSeek-V2-Lite [10] and Mixtral [22], due to their competitive performance and widespread adoption.

Datasets To evaluate model performance, we report normalized zero-shot or few-shot accuracy on the LM-Harness benchmark. The number of shots for each task is detailed in Table 4, which includes multiple tasks: ARC-C [7], BoolQ [6], HellaSwag [43], MMLU [20], OBQA [30], PIQA [2], RTE [40], WinoGrande [1] and GSM8K [8]. The evaluation code is based on EleutherAI’s LM Harness framework [16].

Table 4: **Experimental settings for evaluation tasks.** “Norm” refers to the normalization performed with respect to the length of the input.

Task	Number of few-shot	Metric
BoolQ	0	Accuracy
RTE	0	Accuracy
OBQA	0	Accuracy (Norm)
PIQA	0	Accuracy (Norm)
MMLU	5	Accuracy
WinoGrande	5	Accuracy
GSM8K	5	Exact Match
HellaSwag	10	Accuracy (Norm)
ARC-C	25	Accuracy (Norm)

B Multi-Modal Tasks

In the scope of this paper, multimodal tasks refer to those involving both vision and language modalities. We evaluate model performance using three representative benchmarks: MME, MMBench, and SEED-Bench, each targeting different aspects of multimodal understanding and reasoning.

MME benchmark evaluates vision-language models along two dimensions: perception, which tests visual grounding and recognition, and cognition, which assesses reasoning abilities such as counting and relational understanding. It provides a fine-grained analysis of multimodal understanding.

MMBench is a comprehensive benchmark designed to assess the general multimodal understanding ability of vision-language models. It evaluates model performance across six core capabilities: Coarse Perception (CP), Fine-grained Perception—including single-instance (FP-S) and cross-instance (FP-C), Attribute Reasoning (AR), Logical Reasoning (LR), and Relational Reasoning (RR). By covering both perception and reasoning-oriented tasks, MMBench provides detailed insights into the strengths and limitations of VLMs across diverse multimodal scenarios.

SEED-Bench is a large-scale benchmark for evaluating the generative comprehension of Multimodal Large Language Models (MLLMs) across both image and video modalities. It includes 19K human-annotated multiple-choice questions spanning 12 evaluation dimensions, enabling objective and efficient assessment without human or GPT intervention. SEED-Bench reveals model limitations and maintains a public leaderboard to support fair comparison and future research.

Component	Content	Token Count
Image		576
Text Prompt	Is this artwork titled virgin and child with sts catherine, cecilia, barbara, and ursula? Please answer yes or no.	31
Total	-	607

Table 5: An example multi-modal query in MME benchmark, showing the dominant proportion of image tokens compared to text tokens.

As shown in Table 5, these tasks typically introduce a large number of image tokens. When faced with imbalanced token-to-expert assignments, dropping redundant image tokens significantly improves

load balancing. Moreover, due to the high redundancy among image tokens, dropping a portion of them has minimal impact on model performance.

As in MME and MMBench, the Image-First variants of Token Drop and Expanded Drop also exhibit consistent effectiveness on SEED-Bench [27], maintaining strong performance even under low capacity factors such as $\gamma = 0.5$. In addition to the redundancy in image tokens, Figure 9 shows that text tokens constitute only a small portion of the total token assignments. This allows the regulation of γ to retain almost all text tokens under the Image-First strategy.

Method	γ	Inst. Attr.	Inst. ID	Inst. Interact.	Inst. Loc.	Inst. Count	Scene	Spatial	Text	Reasoning	Overall
Baseline	∞	74.2	71.4	58.8	62.8	57.0	73.5	49.6	72.6	76.4	68.7
Token Drop	0.5	70.4	67.8	60.8	57.8	51.8	71.5	43.5	58.3	71.3	64.9
Expanded Drop		71.2	67.3	57.7	58.8	53.6	71.0	45.2	64.3	71.9	65.5
Token Drop	1.0	73.6	70.2	58.8	62.6	56.9	72.7	48.1	61.9	73.4	68.0
Expanded Drop		73.8	70.7	59.8	63.5	56.7	73.1	49.6	70.2	74.6	68.4
Token Drop	1.5	73.5	71.2	58.8	62.9	57.1	73.1	48.7	65.5	74.6	68.3
Expanded Drop		73.7	71.0	61.9	64.7	57.4	73.3	49.3	71.4	76.1	68.7

Table 6: Token Drop and Expanded Drop strategies for multi-modal MoE models evaluated on SEED-Bench. Abbreviations: Inst. Attr. = Instance Attributes; Inst. ID = Instance Identification; Inst. Interact. = Instance Interaction; Inst. Loc. = Instance Localization; Inst. Count = Instance Counting.

C Pseudocode for Token Drop and Expanded Drop

We present the detailed pseudo-code for the algorithm implementations, as shown in Algorithm 1 and Algorithm 2. Both of these two methods adopt the selection metrics of “Score.”

Algorithm 1 Token Drop

Require: `input_tokens, num_tokens, num_experts, k, γ`

```

logits  $\leftarrow G(\text{input\_tokens})$ 
scores  $\leftarrow \text{Softmax}(\text{logits}, \text{dim} = -1)$ 
topk_scores, topk_indices  $\leftarrow \text{TopK}(\text{scores}, k = k, \text{dim} = 1)$ 
topk_masked_scores  $\leftarrow \text{torch.zeros\_like}(\text{logits}).\text{scatter}(1, \text{topk\_indices}, \text{topk\_scores})$ 
topk_map  $\leftarrow \text{torch.zeros\_like}(\text{logits}).\text{int}().\text{scatter}(1, \text{topk\_indices}, 1).\text{bool}()$   $\triangleright \text{Drop Token}$ 
expert_capacity  $\leftarrow \gamma \cdot \frac{\text{num\_tokens} \times k}{\text{num\_experts}}$ 
_, capacity_indices  $\leftarrow \text{TopK}(\text{topk\_masked\_scores}, k=\text{expert\_capacity}, \text{dim}=0, \text{sorted}=\text{False})$ 
capacity_mask  $\leftarrow \text{torch.zeros\_like}(\text{logits}).\text{scatter}(0, \text{capacity\_indices}, 1).\text{bool}()$ 
final_map  $\leftarrow \text{topk\_map} \wedge \text{capacity\_mask}$ 
final_scores  $\leftarrow \text{topk\_masked\_gates} \cdot \text{final\_map}$ 
return final_scores, final_map

```

Algorithm 2 Expanded Drop

Require: `input_tokens, num_tokens, num_experts, k, γ , local_expert_id_list`

```

logits  $\leftarrow G(\text{input\_tokens})$ 
scores  $\leftarrow \text{Softmax}(\text{logits}, \text{dim} = -1)$ 
topk_scores, topk_indices  $\leftarrow \text{TopK}(\text{scores}, k = k, \text{dim} = 1)$   $\triangleright \text{Expand}$ 
local_indices  $\leftarrow \text{torch.tensor}(\text{local\_expert\_id\_list}).\text{repeat}(\text{num\_tokens}, 1)$ 
expanded_indices  $\leftarrow \text{torch.cat}((\text{topk\_indices}, \text{local\_indices}), \text{dim} = 1)$ 
local_scores  $\leftarrow \text{scores}[:, \text{local\_expert\_id\_list}]$ 
expanded_scores  $\leftarrow \text{torch.cat}((\text{topk\_scores}, \text{local\_scores}), \text{dim} = 1)$ 
expanded_masked_scores  $\leftarrow \text{torch.zeros\_like}(\text{logits}).\text{scatter}(1, \text{expanded\_indices}, \text{expanded\_scores})$ 
expanded_map  $\leftarrow \text{torch.zeros\_like}(\text{logits}).\text{int}().\text{scatter}(1, \text{expanded\_indices}, 1).\text{bool}()$   $\triangleright \text{Drop Token}$ 
expert_capacity  $\leftarrow \gamma \cdot \frac{\text{num\_tokens} \times k}{\text{num\_experts}}$ 
_, capacity_indices  $\leftarrow \text{TopK}(\text{expanded\_masked\_scores}, k=\text{expert\_capacity}, \text{dim}=0, \text{sorted}=\text{False})$ 
capacity_mask  $\leftarrow \text{torch.zeros\_like}(\text{logits}).\text{scatter}(0, \text{capacity\_indices}, 1).\text{bool}()$ 
final_map  $\leftarrow \text{expanded\_map} \wedge \text{capacity\_mask}$ 
final_scores  $\leftarrow \text{expanded\_masked\_gates} \cdot \text{final\_map}$ 
return final_scores, final_map

```

D Maximum Expert Selection

Expanded Drop employs overselection and dropping to not only ensure load balance but also improve the utilization of underloaded experts. Although this process may allow some tokens to select more than k experts, Table 7 shows that enforcing a strict k -expert limit is unnecessary: allowing additional expert selections has the potential of enhancing representational capacity, while rigid constraints introduce redundant computations.

Table 7: **Ablation study on limiting the maximum number of k selected experts.** “w/max” and “w/o max” indicate runs *with* and *without* this constraint, respectively. γ is set to 1.0.

m	Method	OBQA	PIQA	RTE	WinoGrande	BoolQ	ARC-C	HellaSwag	MMLU	Avg.
$2k$	w/ max	42.4	75.8	53.2	68.6	72.7	50.3	77.1	47.6	61.0
	w/o max	42.2	75.9	53.4	69.7	73.1	50.3	77.0	47.8	61.2
$3k$	w/ max	42.0	75.6	53.4	69.6	72.7	50.3	77.0	47.4	61.0
	w/o max	42.0	75.6	53.8	69.8	72.9	50.3	77.1	47.6	61.1

E Layer-wise Expert Load

To analyze imbalanced token assignments, we measure the expert load for each expert by tracking the peak expert load while running MoE models on various test datasets. Figure 12, 13, 14 and 15 present the full results for the normalized layer-wise expert load for OLMoE, DeepSeek-V2, Qwen1.5-MoE, and Mixtral-8 \times 7B-Instruct, respectively.

F Calculation Dropped tokens

Based on Equation 12, we calculate the total number of dropped tokens across experts in each layer under different capacity factors, as illustrated in Figures 16, 18, 17, and 19.

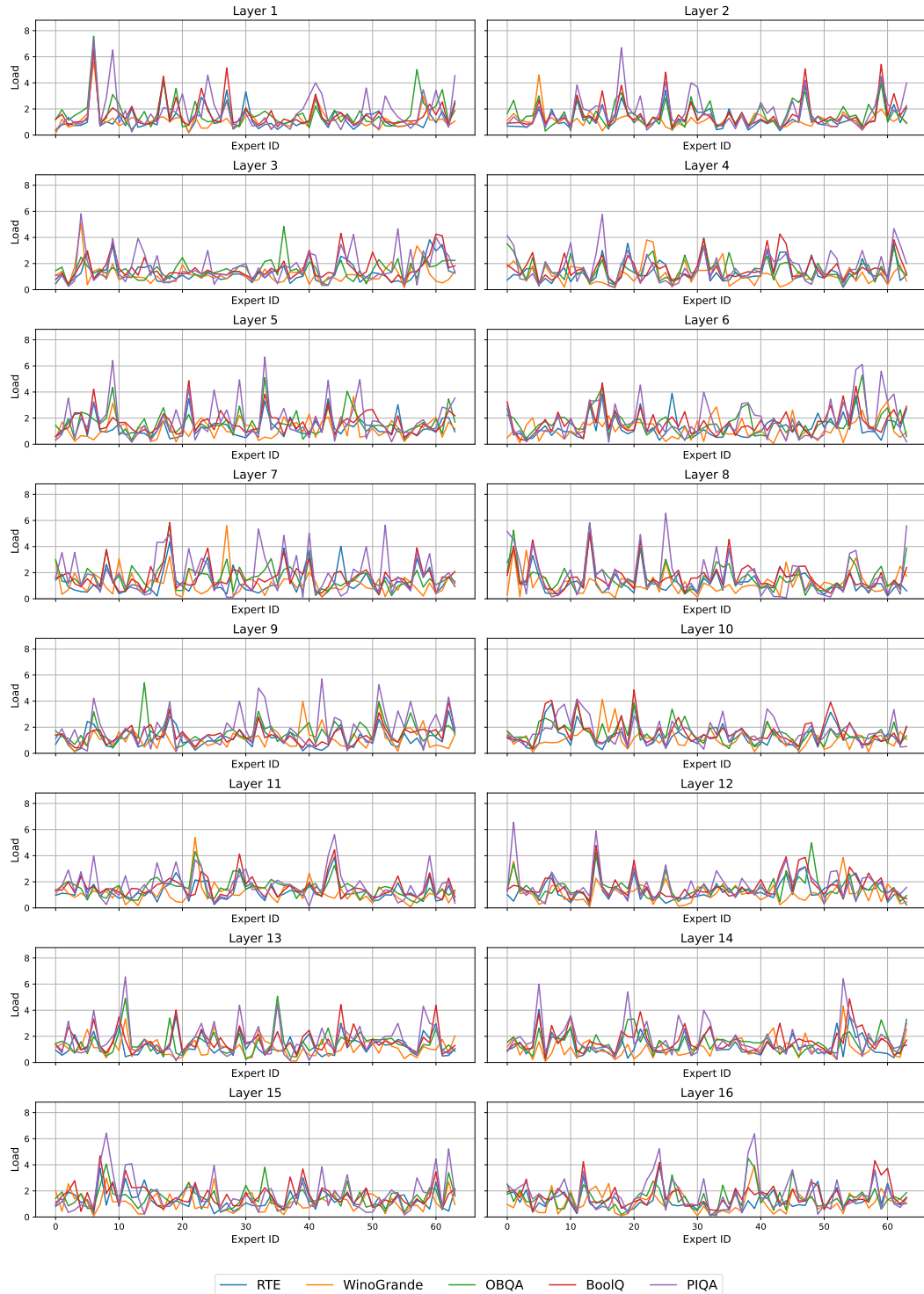


Figure 12: Layer-wise expert load in OLMoE-Instruct.



Figure 13: Layer-wise expert load in Deepseek-V2-Lite.

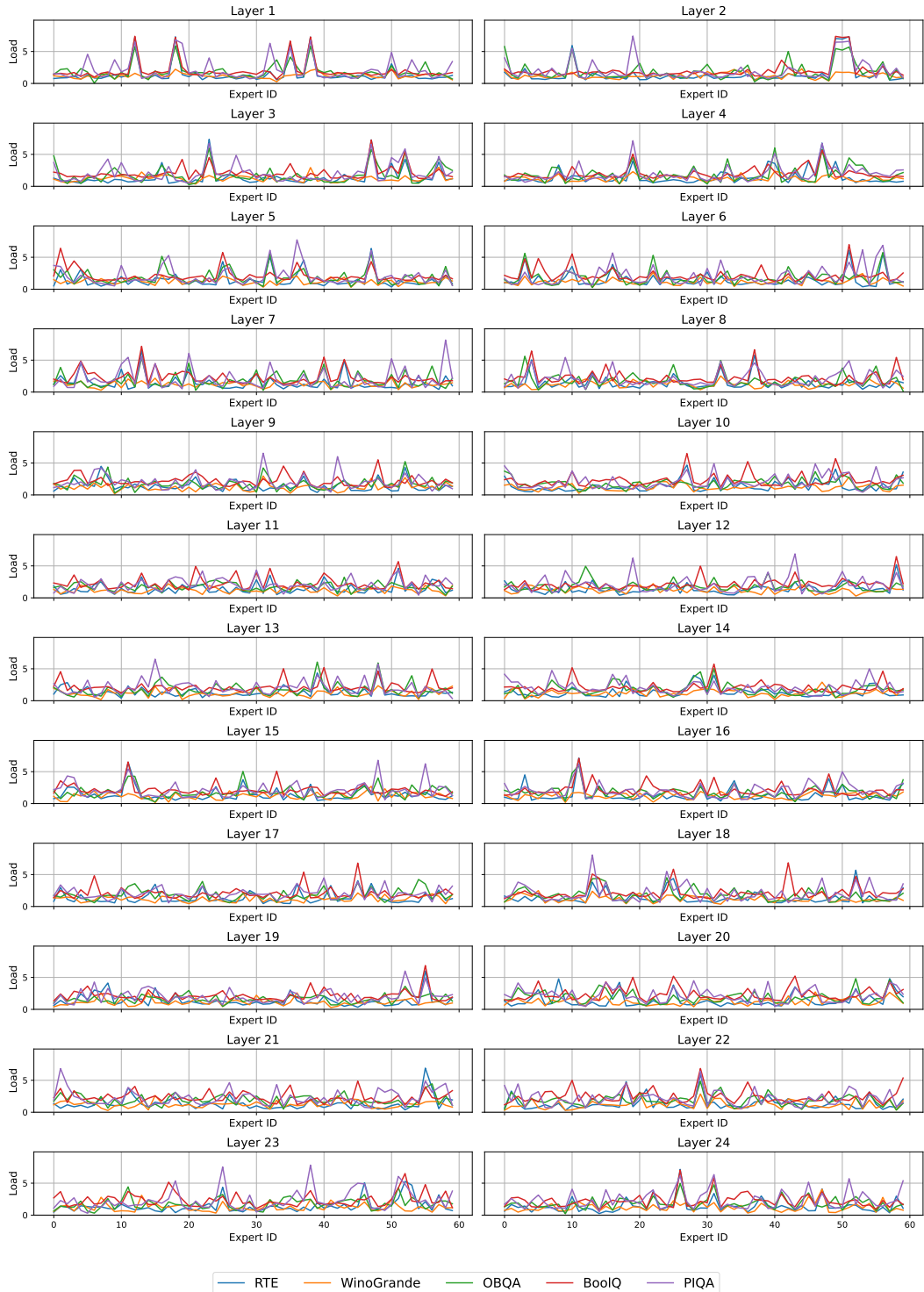


Figure 14: Layer-wise expert load in Qwen1.5-MoE-Chat.

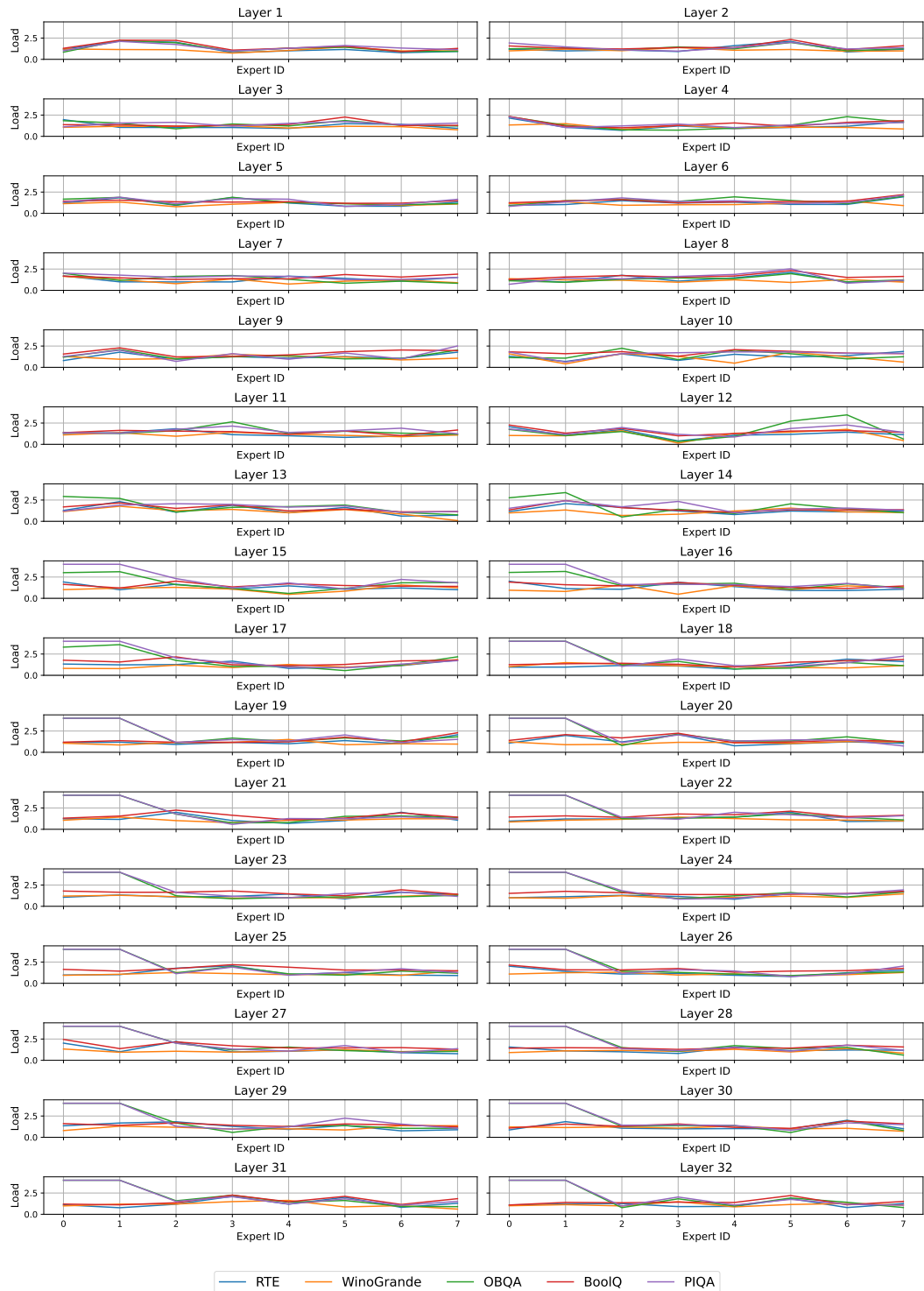


Figure 15: Layer-wise expert load in Mixtral-8 \times 7B-Instruct.

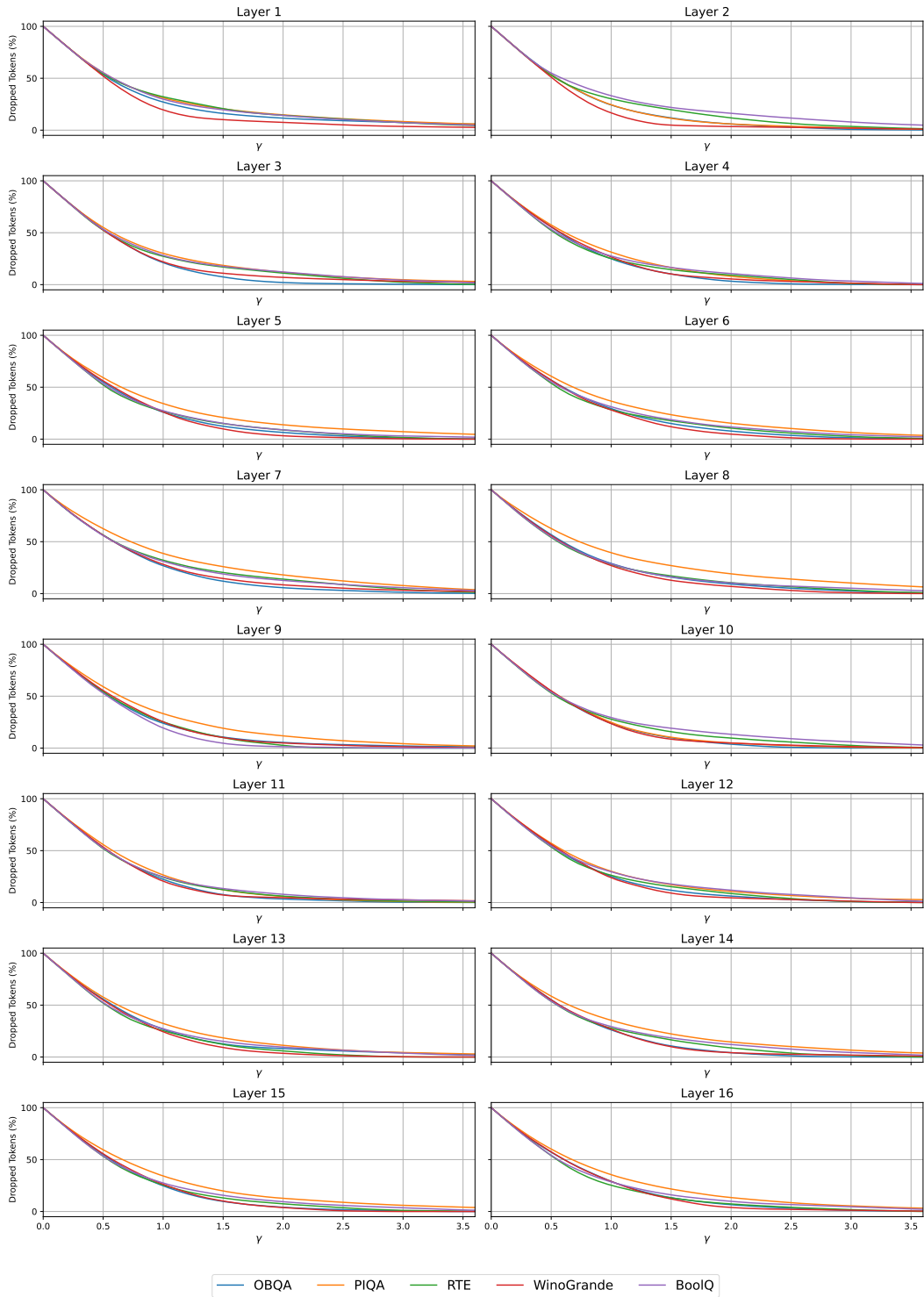


Figure 16: Dropped tokens with respect to capacity factors in OLMoE-Instruct.

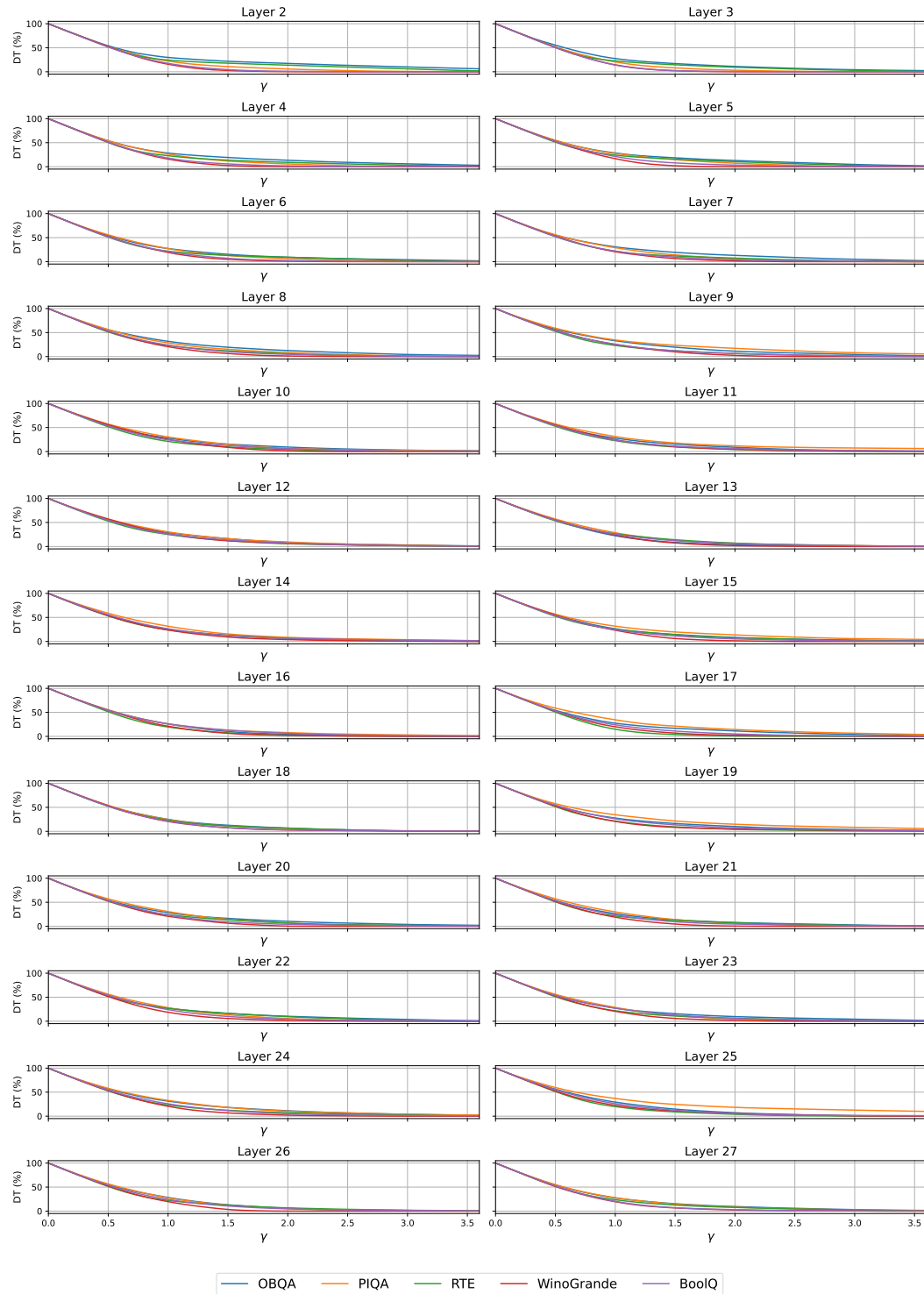


Figure 17: Dropped tokens with respect to capacity factors in DeepSeek-V2-Chat.

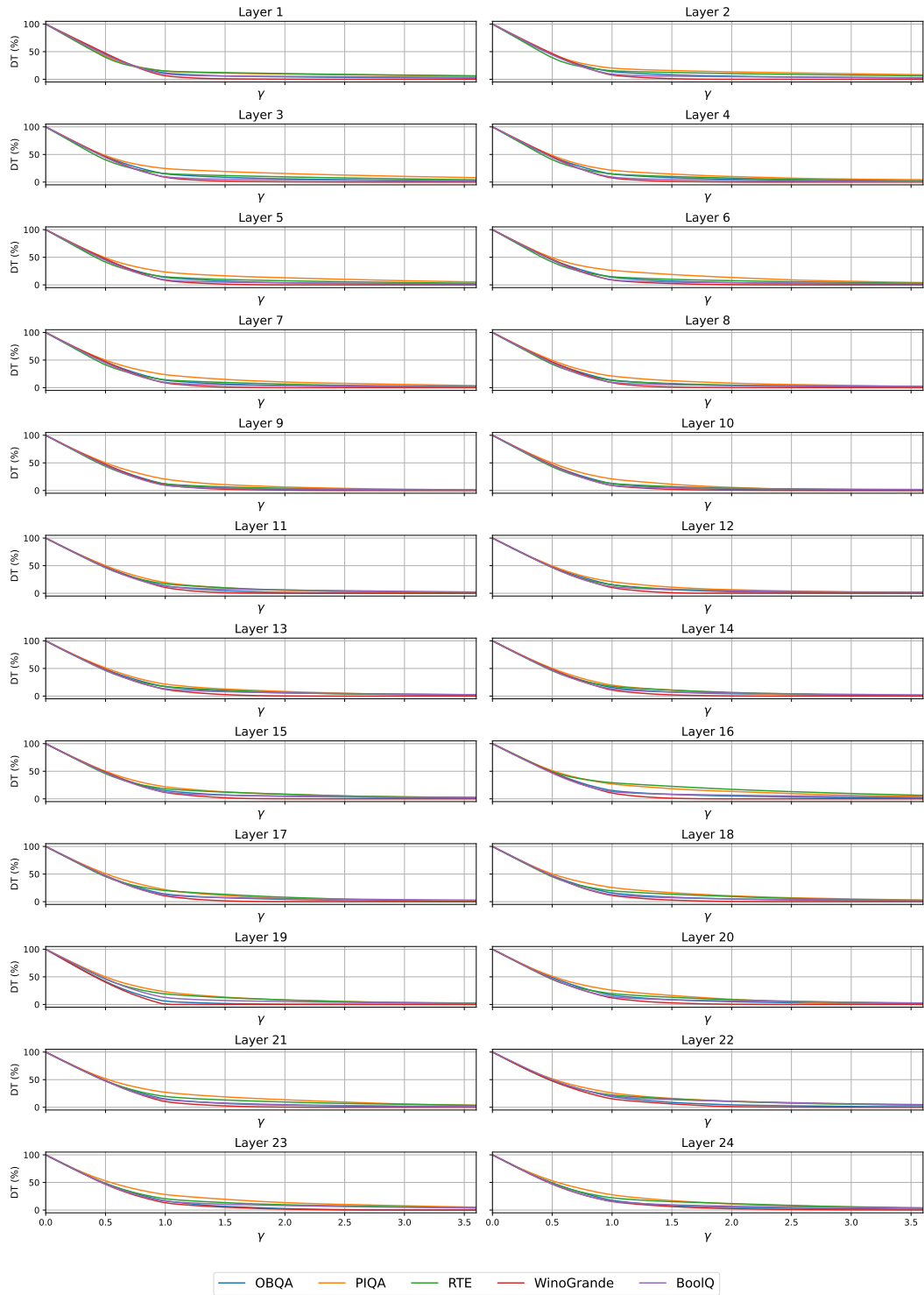


Figure 18: Dropped tokens with respect to capacity factors in Qwen-1.5-MoE-Chat.

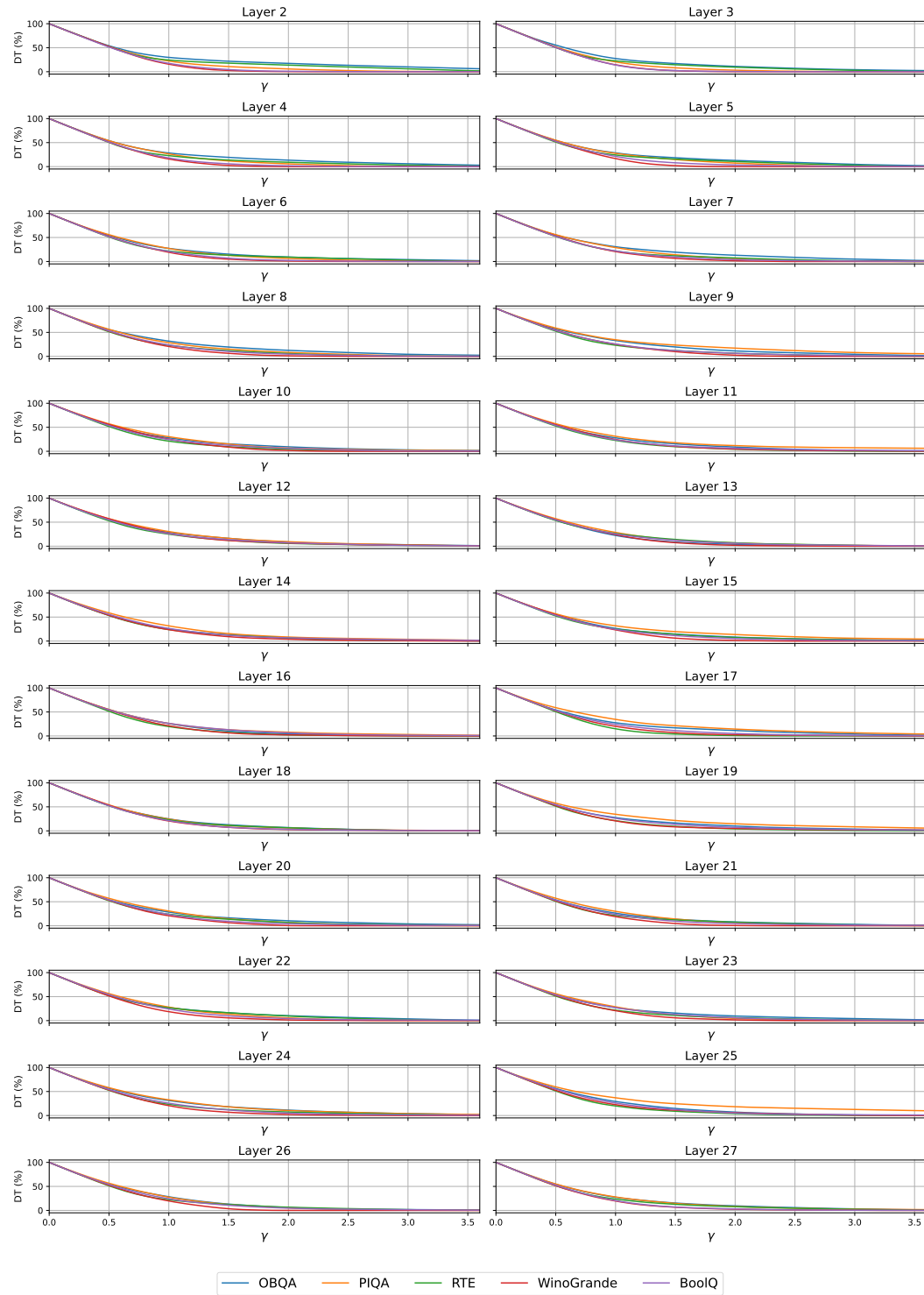


Figure 19: Dropped tokens with respect to capacity factors in Mixtral-8×7B-Instruct.